The multi-functional aspect of scanning holographic microscopy: a review

Invited Paper

Guy Indebetouw

Physics Department, Virginia Tech, Blacksburg, VA 24061-0435, USA

**E-mail: gindebet@vt.edu*

Received March 5, 2009

Recent developments in scanning holographic microscopy that offer the prospects of new quantitative tools and imaging modalities in bio, micro, and nano sciences are reviewed. The versatility of the method is emphasized. Scanning holography can operate in an incoherent mode for fluorescence imaging, in a coherent mode for quantitative phase imaging, or in a tomographic mode for axial sectioning and rejection of the out-of-focus haze. Possible applications are illustrated with examples, and future prospects are discussed.

OCIS codes: 090.1995, 110.6880, 180.0180, 180.6900.
doi: 10.3788/COL20090712.1066.

1. Introduction

Digital holography is an emerging technique that utilizes modern technology to implement in convenient and often useful ways, ideas that had been proposed during the early days of holography[1,2]. A successful example of this development takes advantage of the availability of high-resolution imaging detectors (charge-coupled device (CCD) or complementary metal-oxide semiconductor (CMOS) chips) to record the hologram, and of deep digital memory and powerful processing algorithms to reconstruct and manipulate the holographic data[3]. The application of digital holography to microscopy has the distinct advantage that it gives access to a quantitative measure of the phase of the object[4,5]. The phase information is invaluable for characterizing changes of thickness, density, or refractive indices in unstained living cells, for example. However, one limitation of digital holographic microscopy is that it requires recording the interference of the light scattered by the specimen with a mutually coherent reference beam[6−11]. This need for spatial and temporal coherence prohibits the holographic recording of incoherently scattered fields such as from fluorescent specimens. Yet fluorescence has become an essential tool in modern biological research. It is also an important diagnostic tool in other fields of micro and nano sciences. Scanning holographic microscopy overcomes this limitation by using a two-pupil interaction method[12] that shifts the phase information needed to capture a hologram from the spatial domain to the temporal domain[13,14]. The drawback is that a two-dimensional (2D) scan with a temporally modulated three-dimensional (3D) interference pattern is required to realize the spatial-to-temporal transformation. The pattern is usually a Fresnel pattern obtained with a point and a spherical wave as pupils. It should be mentioned that a scanless incoherent digital holographic method has recently been developed[15]. It has been shown that scanning holographic microscopy offers a number of benefits in addition to being able to capture the 3D holographic information of incoherently scattering specimens. Perhaps the most significant benefit is that scanning holography can operate in an incoherent mode or a coherent mode simply by varying the detector size[16]. The incoherent mode uses a spatially integrating detector and leads to a hologram of the 3D incoherently scattered intensity of the specimen (for example the 3D distribution of fluorophores)[17,18]. The coherent mode uses a pinhole detector placed on axis in the conjugate image plane of the point pupil, and leads to a hologram of the complex amplitude of the specimen from which quantitative phase information can be measured[19]. An equally significant attribute of scanning holography is that it can operate either in a holographic mode or in an axially sectioning tomographic mode by varying the size of the source[20]. With a spatially coherent (point) source, the fringes of the scanning interference pattern are not spatially localized, and the entire 3D scattering distribution of the object is recorded holographically. With a broad, spatially incoherent source filling the pupil of the objective, the interference fringes are axially localized in the focal plane of the objective, and the collected modulated signal represents the hologram of a single tomographic section through the specimen. Firstly, the method of scanning holographic microscopy is briefly reviewed. Various examples illustrating the versatility and possibility of the method are then discussed. Finally, a brief summary and mention of future prospects concludes the paper.

2. Holographic modes

Scanning holographic microscopy has been described in several papers and books[16,21]. The main idea is to create a spatially structured interference pattern, modulate it in time, and scan it in a 2D raster over the specimen. In its simplest implementation, which leads to the recording of an in-line single-sideband Gabor hologram, the interference of a plane wave and a spherical wave matching the numerical aperture (NA) of the objective is used to produce a Fresnel zone interference pattern (FZP)[22,23]. The temporal modulation needed to shift the holographic phase from the spatial to the temporal domain is achieved by shifting the frequency of one of the interfering waves using an acousto-optic or an electro-

optic device. A generic setup is sketched in Fig. 1. The beam from a laser is split into two parts. One part is frequency shifted by an electro-optic phase modulator driven by a saw-tooth waveform. The two beams are expanded to create two pupil distributions $\tilde{P}_1$ and $\tilde{P}_2$ (here they are a point source and a spherical wave), and are recombined collinearly by a beam splitter (BS). The two superposed beams are projected through the afocal system formed by lenses L_1 and L_2 onto the pupil of the objective. The dynamic interference pattern, reduced in size by the afocal system formed by lens L_2 and the objective, is projected through the objective on the specimen. The specimen is scanned in a 2D raster. Different detectors collect the fluorescence and absorbance signal (incoherent mode), and the amplitude transmittance signal (coherent mode) as shown. The data corresponding to each scan line are captured by an analog-to-digital (A/D) acquisition system and demodulated in Fourier space. A reference signal is used to realign the initial phase of each line, and the lines are arranged in a 2D format to form a single-sideband in-line hologram of the specimen. The holograms can be reconstructed by digital Fresnel propagation or by digital correlation with the hologram of a sub-resolution point object recorded experimentally. The latter allows for the immediate cancellation of the system's aberrations, without the need of post-processing, and is not limited to the small angle approximation often implied in the Fresnel-Kirchhoff formulation of the diffraction integral.

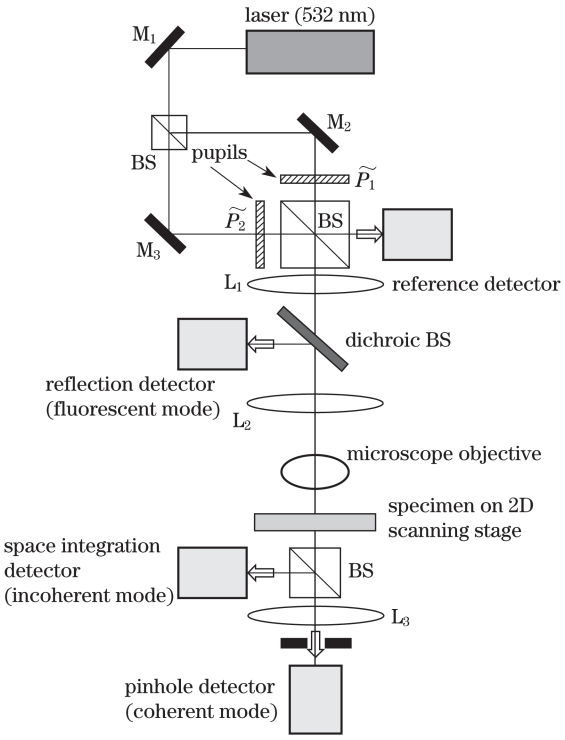

Fig. 1. Sketch of a generic scanning holographic microscope. The upper part is a two-wave interferometer combining two pupil distributions (possibly generated by two spatial light modulators (SLMs)) with a frequency offset to project a temporally modulated interference pattern through the objective on the specimen. The pattern is scanned in a 2D raster. The modulated scattered light is detected in transmission or reflection by spatially integrating detectors to obtain incoherent holograms of the specimen intensity absorbance, reflectance, and fluorescence. A pinhole detector in a conjugate image plane of the pupil of the objective gives a coherent hologram of the complex amplitude transmittance of the specimen from which quantitative phase information can be measured. Replacing the 2-beam interferometer by a Fabry-Perot interferometer illuminated by an extended spatially incoherent source provides axially localized fringes and leads to the hologram of a single axial tomographic section through the specimen.

3. Incoherent mode

To capture holograms of fluorescent samples[18], the temporally modulated scanning Fresnel pattern excites a temporally modulated fluorescence intensity. After projection of the scanning pattern through the objective, detection of the modulated fluorescence signal by a spatially integrating detector, and digital demodulation, an incoherent hologram of the fluorophores scattering intensity distribution is obtained. Typical examples of holographic reconstructions of fluorescent pollen grains are shown in Fig. 2. The resolution of these images is comparable to that of wide-field images obtained with the same objective lens.

Two important properties of the method are worth mentioning. The first is that the instantaneous signal on the detector is the integral of the fluorescence from the entire region excited by the scanning pattern. The size of the scanning pattern is an arbitrary parameter in the instrument design, but it is typically 10 to 100 times the size of the transverse resolution of the objective, which equals the width of the finest outer ring of the Fresnel pattern. This represents a fluorescence signal 100 to 10000 times larger than the signal from a single resolution element, as is detected in wide-field or in confocal microscopy. In scanning holographic microscopy, the signal level is rarely a factor limiting the signal-to-noise ratio (SNR) of the detection system. An additional property

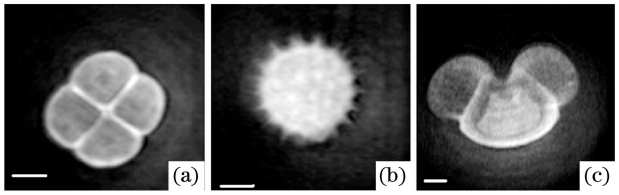

Fig. 2. Reconstructions of the incoherent holograms of typical fluorescent pollen grains. Excitation wavelength is 532 nm, and emission wavelength is 600 nm. The scale bar is 10 μm.

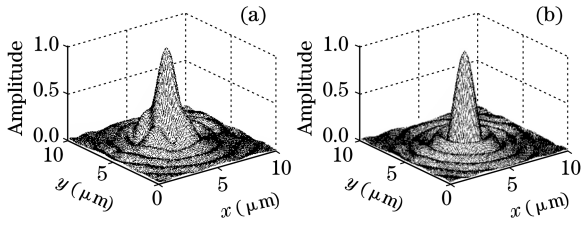

Fig. 3. Experimental PSF of the holographic reconstructions obtained with (a) digital Fresnel propagation from the hologram and (b) correlation with the experimental hologram of a sub-resolution (0.5 μm) pinhole. The latter method effectively cancels the aberrations of the optical system.

is that the aberrations of the optical system are automatically cancelled out if the hologram is reconstructed by digital correlation with the hologram of a sub-resolution point object (pinhole or bead). The reference hologram needs to be recorded only once for a given objective and scanning pattern. It contains the same aberrations as the hologram of the specimen, and the correlation operation cancels out all phase distortions. Figure 3(a) shows the point-spread-function (PSF) of the holographic microscope with reconstruction by digital Fresnel-Kirchhoff propagation. Figure 3(b) is the PSF of the same optical system with reconstruction by correlation with the experimental hologram of a sub-resolution point object. The residual spherical aberration and astigmatism of the former have been effectively cancelled in the latter.

4. Coherent mode

When the signal is captured in transmission by a point detector located on-axis in a conjugate image plane of the pupil of the objective (Fig. 1), the hologram is that of the complex amplitude transmittance of the specimen[19]. In this operation mode, the phase of the reconstruction is the phase transmitted by the specimen integrated axially. It contains information of the sample thickness and refractive index distribution. Figure 4 shows the amplitude and phase of the reconstruction of a Spongila Spicule which is essentially a colorless organic calcite crystal. Quantitative morphology can be measured from such data.

The accuracy of the phase information obtained by this holographic method was tested by comparing the profile of a 110 line/mm triangular epoxy phase grating obtained from the phase of the holographic reconstruction with the profile obtained directly with an atomic force microscope (AFM). The disagreement shown in Fig. 5 is within 5%.

Co-localization of sub-resolution fluorescent markers is a powerful tool in cell biology as it provides a means of correlating functional behaviors with morphological structures. 2D co-localization is achieved routinely by measuring the position of the centroids of the marker images, but 3D co-localization remains problematic.

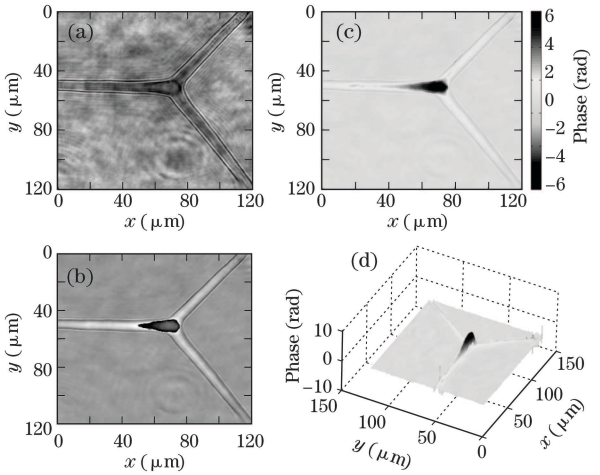

Fig. 4. Reconstruction of the coherent hologram of a transparent Spongila Spicule. (a) Amplitude transmittance; (b) wrapped phase; (c), (d) unwrapped phase.

The reconstruction of a scanning digital hologram is a complex function even if the hologram is recorded in the incoherent mode. Remarkably, the phase of the reconstruction of a sub-resolution object such as a fluorescent marker is exactly proportional to its axial position measured from the plane of focus of the reconstruction, and can be measured with sub-micron accuracy[24]. The method was tested quantitatively using a collection of 1-μm diameter fluorescent beads, a size approximately equal to the transverse resolution of the objective. Figure 6 shows the reconstructed amplitude and phase focused in two planes at respective distances of 3 and 15 μm from the focal plane of the objective. The axial locations of the beads, calculated from the phase of the reconstructions, are indicated in the figure. The method is characterized by two adjustable parameters, the sensitivity $\mathrm{d}\Phi/\mathrm{d}z = (-\pi/2)(\mathrm{NA})^2/2\lambda$, and the free-axial-range $(\Delta z)_{\mathrm{MAX}} = \lambda/(\mathrm{NA})^2$, where Φ is the phase of the reconstruction, NA is the numerical aperture of the scanning pattern, and λ is the wavelength of the excitation radiation[24].

5. Tomographic mode

The holographic mode of operation illustrated in the previous examples has the evident advantage of capturing a 3D volume in a single acquisition step. The reconstructed 3D information may however be corrupted by the out-of-focus haze that also plagues wide-field microscopy. The haze is due to the low spatial frequencies of out-of-focus features, which are always transmitted by the objective and cannot be directly separated from the focused image of interest. Different methods have been successful in combating this problem. For example, deconvolution methods use iterative post-processing algorithms[25]. Confocal imaging prevents the out-of-focus light from reaching the detector, but requires a 3D point-to-point scan and often suffers from low SNR[26]. Wide-field structured illumination uses several phase-stepped frames to obtain the desired in-focus information algebraically[27] or statistically[28]. Scanning holography is also capable of selecting the information scattered by a single axial section of the specimen[20]. To achieve this, the interference fringes of the scanning pattern must be

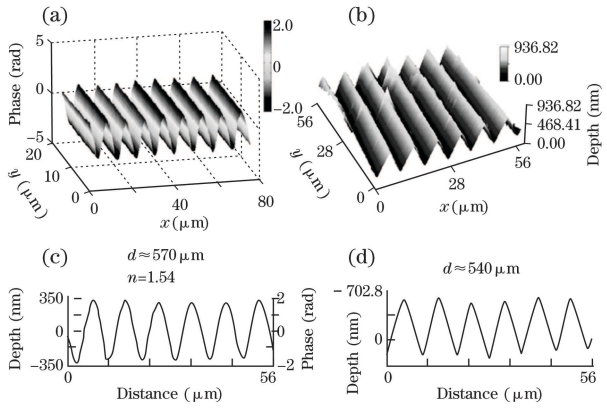

Fig. 5. (a) Phase of the reconstruction of the coherent hologram of a relief phase grating with a 7° triangular profile; (b) profile of the same grating obtained with an AFM; (c) quantitative comparison of the profiles obtained by the AFM (right) and the holographic method (left).

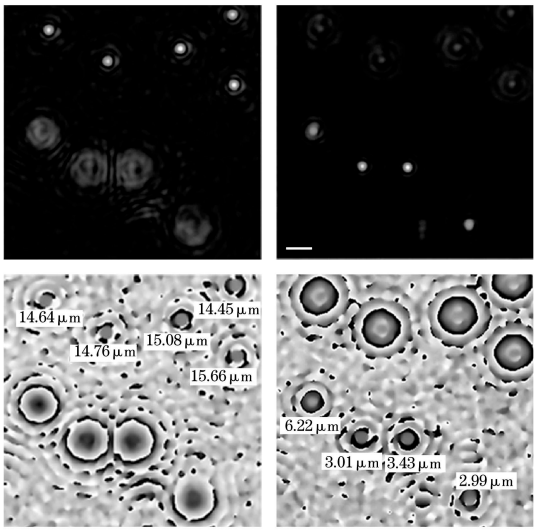

Fig. 6. Reconstructions of the incoherent hologram of a collection of fluorescent beads (1-μm diameter). Excitation wavelength 532 nm, emission wavelength 600 nm, objective 20×, NA=0.4. Left: amplitude (top) and phase (bottom) of the reconstruction focused in a plane 3 μm from the focal plane of the objective. Right: amplitude and phase of the reconstruction focused in a plane 15 μm from the focal plane of the objective. The axial location of the beads is a linear function of the phase of the reconstruction, and can be measured with nanometer accuracy.

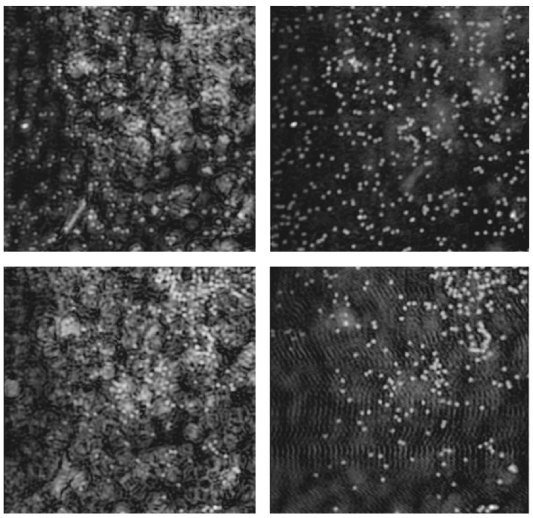

Fig. 7. Left column: reconstruction of the hologram of a dense sample of 2-μm diameter fluorescent beads obtained with a point source and a Fabry-Perot interferometer (excitation wavelength 532 nm, emission wavelength 600 nm). Top: reconstruction focused 15 μm above the focal plane of the objective. Bottom: reconstruction focused 20 μm below the focal plane of the objective. The non-localized scanning pattern captures the hologram of the entire 3D distribution, but the reconstructions are severely corrupted by the out-of-focus features. Right column: reconstruction of two holograms of the same sample obtained with an extended spatially incoherent source. The localized fringes capture the hologram of a single axial section without corruption from the out-of-focus information. Image size: $140\times140\mu m^2$.

spatially localized in the desired axial plane of the specimen. One way to realize axial localization of interference fringes is to use an extended spatially incoherent source instead of the laser shown in Fig. 1. The two-beam interferometer in Fig. 1 can also be replaced by a Fabry-Perot interferometer to simplify alignment. Multiple reflections in the Fabry-Perot cavity (made of two plane parallel partially reflecting mirrors) duplicate each point source in a series of images axially spaced by twice the mirror spacing. The scanning pattern is the incoherent superposition of the Fabry-Perot rings due to each point source. Because the rings due to different point sources overlap exactly only in the back focal plane of the objective, the scanning interference pattern is strictly localized in that particular axial plane. A linear translation of one of the Fabry-Perot mirrors creates a Doppler frequency shift of the reflected wave, which temporally modulates the fringes of the scanning pattern. Consequently, the signal modulated at the Doppler frequency represents the hologram of the axial section of the specimen coinciding with the plane of fringe localization. Light scattered by out-

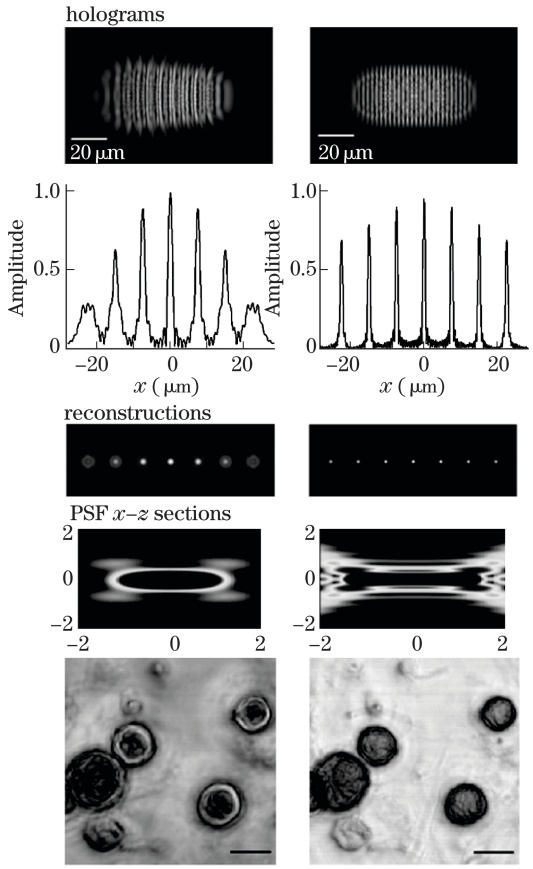

Fig. 8. Left column: hologram obtained with a point and a spherical wave as pupils, leading to a reconstruction identical to a wide-field image using the same objective. Right column: hologram obtained with two spherical waves with opposite curvatures as pupils, leading to a reconstruction with twice the transverse resolution and ten times the DOF of the objective. First row: holograms of seven point objects; second and third rows: reconstructions focused on the central point; fourth row: $x-z$ sections of the corresponding PSF in units of transverse and axial resolution of the objective; fifth row: reconstructions of a Mucor Zygote sample from a conventional hologram (left) and a hologram with extended DOF (right).

of-focus features is not temporally modulated and does not contributes to the signal, although it may tax the dynamic range of the detector. If the image of the extended source fills entirely the pupil of the objective, the axial width of the extracted section equals the depth-of-focus (DOF) of the objective ($\Delta z = \lambda/(\mathrm{NA})^2$). With a source of a smaller size, the width of the section increases as the inverse of the angular size of the source, up to the limit of a single point source with which the fringes are not axially localized and the entire 3D specimen distribution is captured holographically.

Figure 7 illustrates the phenomenon. The left column shows the reconstructions of a densely packed sample of 2-μm diameter fluorescent beads. The hologram was obtained with non-localized fringes using a single point source. The two reconstructions were obtained by correlation with the hologram of a 0.5-μm pinhole located in the focal plane of the objective and numerically propagated to two planes located respectively at 15 μm below (top row) and 20 μm above (bottom row) the focal plane. These two planes coincide respectively with the top of the slide and the bottom of the cover slip where most of the beads have migrated. With some effort, it is possible to identify in-focus beads in one plane or the other, but the images are severely corrupted by the out-of-focus information. The right column shows the reconstructions of two holograms of the same specimen obtained with localized fringes using an extended spatially incoherent source. For each hologram, the specimen was axially translated by respectively –15 and +20 μm from its original position in order to bring the focal plane of the objective (the plane of fringe localization) in coincidence with the two planes where most of the beads are located. This result illustrates the possibility of tomographic imaging without the corruption of the out-of-focus features.

6. PSF engineering

Using a Fresnel zone pattern to scan the specimen leads to a conventional single-sideband Gabor hologram, but scanning holography is not limited to this choice[29]. Spatial light modulators (SLMs) can be used to generate arbitrary complex pupil distributions and synthesize arbitrary scanning interference patterns. Scanning holography is thus not limited to the imaging PSF of the objective, but offers a wide range of possibilities for shaping the imaging property of the microscope to meet desired needs[30]. As a simple example, Fig. 8 compares the results obtained using a point and a spherical wave as pupils (left column) with those obtained using two spherical waves with opposite curvatures (right column) to obtain an extended DOF[31]. The first row shows the numerical holograms of seven point objects axially distant from each other by half the DOF of the objective. The second and third rows show the numerical reconstructions focused on the central point. The fourth row shows x-z sections of the respective PSFs, and the fifth row shows the reconstructions of the experimental hologram of a Mucor Zygote sample. The conventional hologram (left column) gives a reconstruction with resolution and DOF equal to those of the objective. The out-of-focus point images are smeared but contain the same total power as the focused images and are responsible for the out-of-focus haze. One possible way of combating this problem is to extend the DOF of the imaging system. The interference of two spherical waves with opposite curvatures varies as the square of the defocus distance, as opposed to the linear dependence of the interference of a spherical wave and a plane wave. Consequently, the scanning interference pattern is, to first order, independent of defocus, and the DOF of the reconstruction can be extended controllably. In the example shown, the DOF is ten times of that of the objective. In addition, if both waves match the NA of the objective, their interference creates a scanning Fresnel distribution with twice the NA of the objective. The transverse resolution is thus expected to be twice that of the objective as verified in Fig. 8.

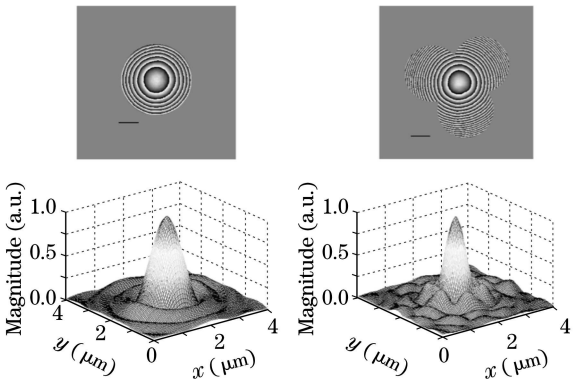

Fig. 9. Experimental PSF of the holographic reconstructions obtained with a single on-axis hologram (left column) and the tiling of three off-axis holograms obtained with the same objective (right column). Top row: wrapped phase of the scanning distributions; bottom row: PSF of the reconstructions, identical to that of the objective in the former case, and exceeding the Rayleigh limit of the objective by a factor of two in the latter case.

Figure 9 illustrates another PSF manipulation intended to increase the resolution beyond the Rayleigh limit of the objective by tiling a number of off-axis holograms to obtain a pupil with an extended area[32].

7. Summary

Several potentially useful features of scanning holographic microscopy have been briefly reviewed. Emphasis is given to the multi-modal possibility of the method. It is shown that with a spatially coherent (point) source and a spatially integrating detector, the method operates in an incoherent mode capable of capturing holograms of 3D incoherently scattered field intensity such as fluorescence distributions. With a point source and a pinhole detector, the method operates in a coherent mode, capturing holograms of complex amplitude distributions from which quantitative phase information can be measured. With an extended incoherent source, the fringes of the scanning interference pattern are localized in a specific axial plane, and the hologram is that of a specific axial section of the specimen, allowing tomographic imaging. The possibilities of the method are far from having been exhaustively explored. Current studies include the use of arc sources with extended wavelength diversity and the use of low coherence broadband sources. One particular area in need of improvement is the acquisition rate of

the method which is presently limited by the 2D scan. As the performance of resonant mirror scanner improves, the hope is to reach an acquisition rate of several tens of holograms per second, each hologram representing a volume of up to 10^6 voxels. The possibility of scanning only one of the beams to improve speed has also been explored by others[33].

I wish to thank the editor T.-C. Poon for inviting me to write this review. I am particularly indebted to all my students who have contributed to this work. A list would be too long, but their names appear in the cited references. The financial support for this work came, in part, from grants from the National Science Foundation and from the National Institute of Health of USA.

References

1. J. W. Goodman and R. W. Lawrence, Appl. Phys. Lett. **11,** 77 (1967).
2. M. A. Kronrod, N. S. Merzlyakov, and L. P. Yaroslavskii, Sov. Phys. Techn. Phys. **17,** 333 (1972).
3. U. Schnars and W. P. O. Juptner, Meas. Sci. Technol. **13,** R85 (2002).
4. E. Cuche, F. Bevilaqua, and C. depeursinge, Opt. Lett. **24,** 291 (1999).
5. E. Cuche, P. Marquet, and C. Depeursinge, Appl. Opt. **38,** 6994 (1999).
6. D. Gabor, Nature **161,** 777 (1948).
7. D. Gabor, Proc. Roy. Soc. London A **197,** 454 (1949).
8. D. Gabor, Proc. Phys. Soc. B **64,** 44954 (1951).
9. E. N. Leith and J. Upatnieks, J. Opt. Soc. Am. **52,** 1123 (1962).
10. E. N. Leith and J. Upatnieks, J. Opt. Soc. Am. **54,** 1295 (1964).
11. E. N. Leith, J. Upatnieks, and K. Haines, J. Opt. Soc. Am. **55,** 981 (1965).
12. A. W. Lohmann and W. T. Rhodes, Appl. Opt. **17,** 1141 (1978).
13. T.-C. Poon and A. Korpel, Opt. Lett. **4,** 317 (1979).
14. T.-C. Poon, J. Opt. Soc. Am. A **2,** 521 (1985).
15. J. Rosen and G. Brooker, Nature Photon. **2,** 190 (2008).
16. G. Indebetouw, P. K. Klysubun, T. Kim, and T.-C. Poon, J. Opt. Soc. Am. A **17,** 380 (2000).
17. B. Schilling, T.-C. Poon, G. Indebetouw, B. Storie, K. Shinoda, and M. Wu, Opt. Lett. **22,** 1506 (1997).
18. G. Indebetouw and W. Zhong, J. Opt. Soc. Am. A **23,** 1699 (2006).
19. G. Indebetouw, Y. Tada, and J. Leacock, BioMed. Eng. OnLine **5,** 63 (2006).
20. G. Indebetouw, J. Opt. Soc. Am. A **26,** 252 (2009).
21. T.-C. Poon, "Optical scanning holography: principles and applications" in C. J. Kuo and M. H. Tsai, (eds.) *Three-Dimensional Holographic Imaging* (Wiley, New York, 2002).
22. G. L. Rogers, Nature **166,** 237 (1950).
23. G. L. Rogers, Proc. Roy. Soc. Edinburgh **513,** 193 (1962).
24. G. Indebetouw, J. Opt. Soc. Am. A **23,** 2657 (2006).
25. P. Sarder and A Nehorai, IEEE Signal Process. Mag. **23,** (3) 32 (2006).
26. J. B. Pawley, (ed.) *Handbook of Biological Confocal Microscopy* (Plenum Press, New York, 1995).
27. M. A. A Neil, R. Justaikis, and T. Wilson, Opt. Lett. **22,** 1905 (1997).
28. C. Ventalon and J. Mertz, Opt. Express **14,** 7198 (2006).
29. G. Indebetouw, J. Mod. Opt. **49,** 1479 (2002).
30. G. Indebetouw, A. El Maghnouji, and R. Foster, J. Opt. Soc. Am. A **22,** 892 (2005).
31. G. Indebetouw, W. Zhong, and D. Chamberlin-Long, J. Opt. Soc. Am. A **23,** 1708 (2006).
32. G. Indebetouw, Y. Tada, J. Rosen, and G. Brooker, Appl. Opt. **46,** 993 (2007).
33. J. Swoger, M. Martinez-Corral, J. Huysken, and E. H. K. Stelzer, J. Opt. Soc. Am. A **19,** 1910 (2002).